

International Journal of Multidisciplinary Research and Growth Evaluation.



Investigation of Corrosion Effects on the Mechanical Resistance of Hydraulic Steel Structures

Danish Iqbal ¹, Muhammad Mujahid ^{2*}, Asif Raza Jarwar ³, Wellington ⁴, Habib Sultan ⁵

- ¹ College of Water Resource and Hydropower Engineering, Hohai University, Nanjing 211100, China
- ^{2,4} College of Hydrology and Water Resources, Hohai University, Nanjing, China, Zip Code 211100
- ³ School of Electrical and Power Engineering, Hohai University, Nanjing, China
- ⁵ Board of Intermediate and Secondary Education, Rawalpindi, Pakistan
- * Corresponding Author: Muhammad Mujahid

Article Info

ISSN (online): 2582-7138

Volume: 05 Issue: 06

November-December 2024 **Received:** 10-11-2024 **Accepted:** 13-12-2024 **Page No:** 1408-1414

Abstract

Corrosion is a key factor affecting the structural safety of hydraulic gates. Through the image recognition technology of the LBP algorithm, the geometric shape information such as the identification unit and the LBP₁₆² value is clarified, and the degree of disease of the corroded component is quantitatively identified. Combined with the resistance bearing test of the corroded components, the resistance performance of the corroded components exhibits a quadratic parabolic attenuation characteristic with the degree of corrosion disease, and the maximum attenuation of the resistance index in the area with severe corrosion disease exceeds 44.41%, and it presents obvious discreteness and uncertainty. It is an effective technical measure to prevent engineering disasters to strengthen the identification of corrosion disease of the stressed components of the gate, especially the disposal or scrapping of the seriously corrosion diseased area.

Keywords: gate, corroded components, degree of corrosion disease, finite element analysis, resistance decay

1. Introduction

Hydraulic steel gate is an important equipment in water conservancy and hydropower projects, which is affected by the operation environment such as dry and wet alternation, and the stressed components of the gate are prone to corrosion. United States California Folsom Dam Spillway No. 3 arc gate was structurally unstable and collapsed during the opening and closing process due to severe corrosion of the arm webs (Jarwar *et al.*, 2023; Li *et al.*, 2024; Todd, 1999) [5, 7, 14]. The severe corrosion of the main beam of the spillway gate of Wangjia'an Reservoir causes the structural bearing rigidity to become smaller, and the structural deformation and water leakage induce serious self-excited vibration diseases (Lu *et al.*, 2023) [9]. Therefore, it is of great engineering significance to strengthen the research on the influence of the mechanical bearing properties of corroded components.

For a long time Li, Saeedikhani, zheng, Granata, S, Tang and other scholars have stated in their related papers (Ang & Tang, 2007; Granata *et al.*, 1996; Li *et al.*, 2022; Mujahid *et al.*; Saeedikhani, 2024; Zeng *et al.*, 2022) [1, 4, 10, 16]. that the failure of the gate stressed member is a complex super static system, and it is difficult to extract the morphological characteristics and geometric information of the surface of the corroded member, and it is difficult to determine the mechanical bearing performance of the corroded member by mechanical test or finite element analysis calculation mechanical method. In recent years, image recognition technology has developed rapidly, and the LBP image recognition algorithm has high accuracy and recognition rate when extracting topographic features. Liu Guanwei (刘贯伟 *et al.*, 2022) and other scholars used the image recognition technology of LBP algorithm to accurately extract the watermark morphology information of RMB, and achieved a good effect of authenticity. Dheepak, Wageh (Dheepak & Vaishali, 2024; Wageh *et al.*, 2023) [3, 15] and other scholars used the image recognition technology combining LBP algorithm and grayscale symbiosis matrix to directly extract grayscale value, entropy,

contrast and other information from tumor images for accurate tumor identification. It can be seen that the application of LBP algorithm It can be seen that the application of LBP algorithm image topography recognition and geometric information extraction technology provides support for the three-dimensional reconstruction and fine modeling of corrosion topography, so as to clarify the resistance attenuation characteristics of corroded components based on finite element analysis and load-bearing test data, and provide rapid identification technology for the safety of in-service gates.

1. Research on the resistance attenuation characteristics of corroded components

The LBP algorithm image recognition technology was used to quickly extract the corrosion morphology information of the corroded components, carry out the three-dimensional reconstruction and fine modeling of the corrosion morphology, and comprehensively evaluate the degree of corrosion disease of the corrosion morphology through multifactor indicators (Liu *et al.*, 2019) [8], and establish the correlation characteristics between the degree of corrosion disease and the resistance performance of the corroded components by combining the finite element bearing test data of the components, so as to clarify the influence of the degree of corrosion disease on the resistance performance of the components, and finally provide a rapid diagnosis technology for the safety of the in-service gate. The resistance attenuation model of the corroded member is shown in Figure 1 and the Figure 2 shows Analytical Flowchart of Corrosion Assessment and Structural Analysis of Steel Gates.

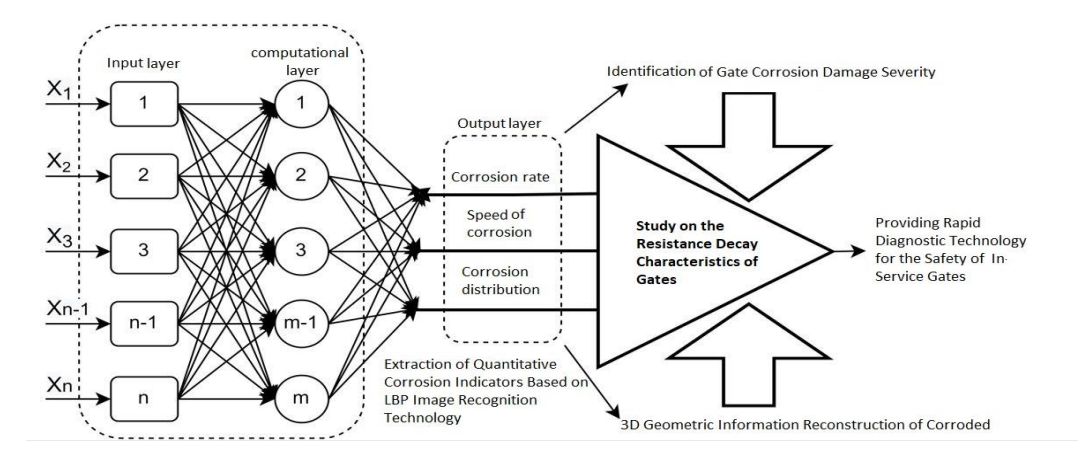


Figure 1: Resistance attenuation model of corroded components

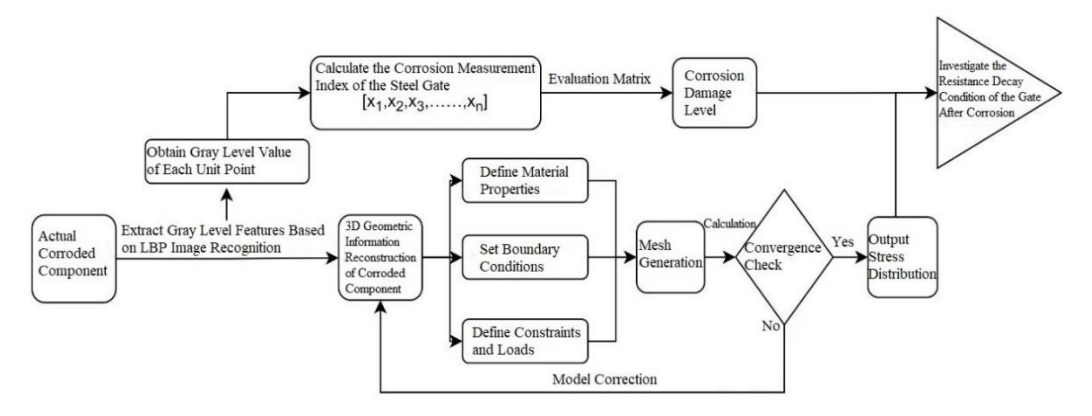


Fig 2: Analytical Flowchart of Corrosion Assessment and Structural Analysis of Steel Gates

1.1 LBP algorithm image recognition technology

LBP is an algorithm that describes the relationship between the gray value of the pixel in the center of the image and the gray value of the pixel in the neighborhood. Any 3*3-pixel tile, with the gray value of the center pixel as the threshold, if the gray value of the surrounding pixels is greater than the threshold, the position is marked as 1, otherwise it is 0, and the 8-bit binary value is used to identify the geometric topography information of the tile (denoted as LBP value). Circular tiles with radius R=2 and pixel P=16 are usually used instead of 3*3 pixel square tiles to better identify geometric topography information (Song *et al.*, 2024), which is denoted as LBP₁₆² (see Equation 1).

$$LBP_{16}^{2} = \sum_{i=1}^{16} \operatorname{sgn}(I(i) - I(c))^{*}2^{i}$$
 (1)

where I(i) represents the gray value of the ith pixel of the circular boundary; I(c) represents the gray value of the center pixel; $sgn(\cdot)$ is a threshold function.

The corrosion image is segmented according to the resolution of 600dpi and 1mm2, and every 25 tiles is 1 identification unit point, 25 LBP $_{16}^2$ values are obtained by formula 1 to replace the gray value of the original block, and according to the principle of normal distribution 1σ , 68.2% of the stress amplitude is selected as the center point to influence the neighborhood, a total of n identification unit points, and 25 LBP $_{16}^2$ values are recorded n×, so that the sharpness, contrast and color resolution of the original image of each identification unit point are significantly enhanced (see Fig. 3).

Fig 3: Corrosion affected area extracted based on LBP algorithm

1.2 Assessment of disease degree in the eroded area

The LBP algorithm was used to directly extract the corrosion morphology information such as the identification unit and LBP $_{16}^2$ value, and combined with statistical methods, the corrosion morphology metrics such as corrosion rate u_1 (the ratio of the weighted mean value of corrosion amount to the design value), corrosion rate u_2 (the ratio of the weighted average value of corrosion amount to the service period) and corrosion distribution u_3 (the relative proportion of the corroded area) were formed, and the comprehensive evaluation of the degree of corrosion disease was carried out according to the multi-index factors (Patil & Shinde, 2015) $^{[11]}$ (see Equation 2).

Combined with the corrosion characteristics of gate components and related standards ("水工钢闸门和启闭机安

全检测技术规程," 2003) [18], the degree of corrosion disease is divided into five grades (v_1 , v_2 , v_3 , v_4 , and v_5), and the measurement indicators of corrosion morphology (u_1 , u_2 , u_3) are shown in Table 1. The fuzzy evaluation matrix [Z] associated with each single factor index and each disease

grade was established, and the evaluation factor of the fuzzy evaluation matrix [Z] was normalized by using the descending half-trapezoidal membership function (Chen *et al.*, 2021) ^[2], and the weight vector W was clarified taking into account the importance of each single factor index, so as to realize the correlation calculation of the Y vector of comprehensive evaluation, and finally determine the degree of corrosion disease according to the principle of maximum membership.

$$\begin{cases}
Y = W \cdot Z \\
Z_{11} \quad Z_{12} \quad Z_{13} \quad Z_{14} \quad Z_{15} \\
Z_{21} \quad Z_{22} \quad Z_{23} \quad Z_{24} \quad Z_{25} \\
Z_{31} \quad Z_{32} \quad Z_{33} \quad Z_{34} \quad Z_{35}
\end{cases}$$
(2)

In the formula, z_{ij} , (i=1,2,3; j=1,2,3,4,5) is the evaluation factor, which reflects the probable degree of the ith corrosion morphology metric relative to the jth grade of the corrosion disease, and is calculated by the half-trapezoidal membership function.

	v ₁ Grade I, slightly corroded	V ₂ GradeII, General corrosion	V ₃ Grade III, Heavy corrosion	V ₄ Grade IV, Severe corrosion	v ₅ Grade V, Rust
u ₁ Corrosion rate/%	≤2	2~6.5	6.5~12	12~20	>20
u ₂ Corrosion rate /mm/a	≤0.01	0.01~0.03	0.03~0.05	0.05~0.06	>0.06
u ₃ Corrosion	≤10	10~30	30~70	70~95	>95

Table 1: Classification standard of factor index and disease grade

				(0	$(x < x_{j-2}, x > x_{j+1})$		
$\begin{pmatrix} 1 \\ x_2 - x \end{pmatrix}$	$(x < x_1)$ $(x_1 < x < x_2)$ $(x > x_2)$	$\begin{pmatrix} 0 \\ x-x_3 \end{pmatrix}$	$(x < x_3)$	$\frac{1}{x}$	$\frac{x-x_j}{x_{i+1}-x_i}$	$\left(x_{j-2} < x < x_{j-1}\right)$	(2)	
$z_{i1} = \begin{cases} \frac{z}{x_2 - x_1} \\ 0 \end{cases}$	$(x_1 < x < x_2)$	$z_{i5} = \begin{cases} \frac{3}{x_4 - x_3} \end{cases}$	$(x_3 < x < x_4)$	$z_{ij_{ j=2,3,4}} = \left\{ \right.$	1	$(x_{j-1} < x < x_j)$	(3)	
(0	$(x > x_2)$	(1	$(x_4 < x)$	$\frac{1}{x}$	$x_{j+1}-x$ $x_{i+1}-x_i$	$(x_j < x < x_{j+1})$		

1.3 Load-bearing performance of corroded components 1.3.1 Model reconstruction of corroded components

According to the geometric information of the erosion topography extracted by LBP, n two-dimensional erosion curve polynomials are established, and lofting them into three-dimensional surfaces, and the bearing models of the erosion surfaces and corrosion components are reconstructed, as shown in Figure 4.

1.3.2 Finite element analysis of the bearing performance of corroded components

The load-bearing tests of the corroded components are carried out by finite element analysis. The image morphology recognition and geometric information extraction technology of LBP algorithm are used to carry out three-dimensional reconstruction and fine modeling of the corrosion morphology of the corroded components (slight corrosion,

general corrosion, heavy corrosion, severe corrosion, rust damage and no corrosion), apply the agreed bearing capacity, analyze the bearing performance data of the corroded components, and obtain the resistance attenuation law of each corrosion-affected area. The load-bearing test is carried out as shown in Figure 4.

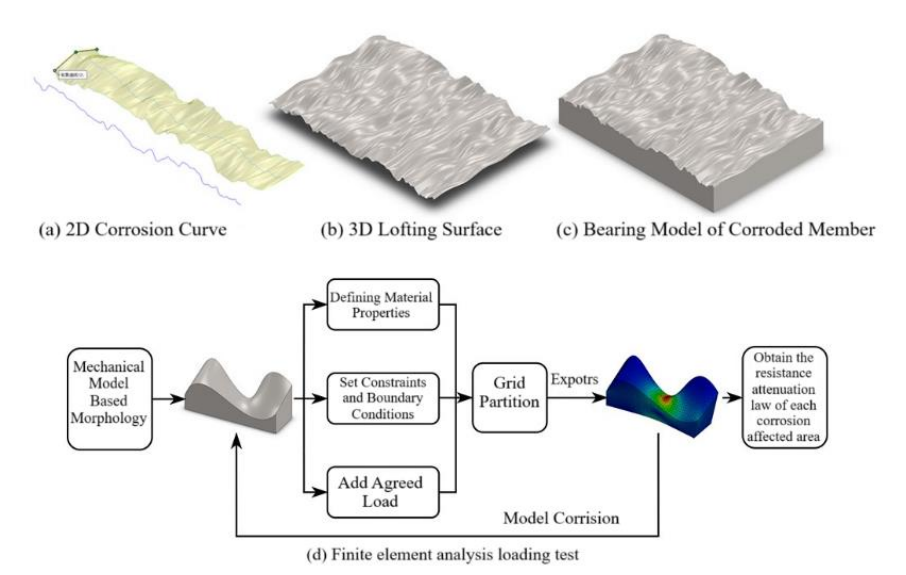


Fig 4: Three-dimensional reconstruction and bearing test of corroded components (a) 2D corroded curve (b) 3D lofted surface (c) bearing model of corroded components (d) finite element analysis bearing test

2. Research on the resistance attenuation characteristics of corroded components

Taking the main beam of the decommissioned gate of a project as the test object, the area size of $40.0 \text{cm} \times 26.0 \text{cm}$ (design thickness value of 2.0 cm) was selected from the web of the corroded main beam, and the image was identified and optimized based on the LBP algorithm to grasp the geometric information of the corrosion morphology of the corroded component (see Fig. 5).

According to the resolution of 600dpi and 1mm^2 , 104,000 identification unit points and $104,000 \times 25 = 2,600,000 \text{ LBP}_{16}^2$ values were obtained from the sampled corrosion image, so that the sharpness, contrast and color resolution of the original image of each identification unit point were significantly enhanced, so as to better identify the geometric

morphology information. The comprehensive evaluation of the degree of erosion disease was carried out according to multiple index factors, and the bearing test of the corroded components was carried out based on the model reconstruction, and finally the resistance attenuation characteristics of the corrosion bearing model were mastered, so as to provide rapid identification technology for the safe operation of the gate of the in-service project. In order to better ensure the objectivity of the bearing test data of the corroded components, we randomly extracted 50 sample points in 5 rows and 10 columns on the images of the sampled corroded components, and marked them as A1~A₅₀ in turn, and the coordinates (x, y) of the sample points and the location information of the affected neighborhood radius R are shown in Table 2.

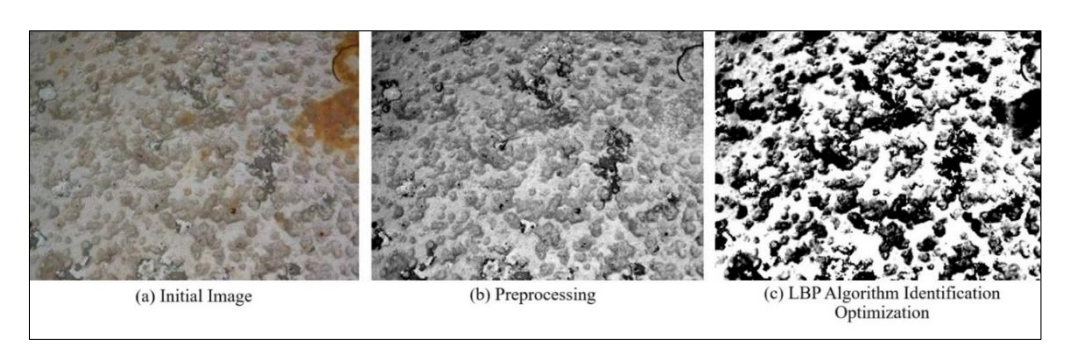


Fig 5: Extraction of corrosion morphology information based on LBP algorithm: (a) initial picture (b) pretreatment (c) identification optimization of LBP algorithm

2.1 Bearing test of corroded components

2.1.1 Reconstruction of the erosion model

Based on the 104,000 identification unit points and 2,600,000 LBP₁₆² values obtained from the images of the corroded components, a one-to-one correspondence between the eroded morphology information and the geometric dimensions was established, and the two-dimensional polynomial curves of 260 corroded surfaces were fitted and lofted out into three-dimensional surfaces with the

reproduction of the corroded complex profile, so as to realize the three-dimensional reconstruction of the bearing model of the corroded component (as shown in Fig. 6).

2.1.2 Load-bearing analysis of corroded components

In order to clarify the bearing performance of the corroded components, the mechanical and static stress simulation analysis of the bearing model was carried out according to the finite element calculation. The material of the bearing model is Q235 steel, the left side of the model adopts fixed constraints, the right side of the model applies the agreed bearing capacity of 400KN, and a total of 2,080,000 grid element points are divided, and the stress response of the corroded component is shown in Figure 6, in which the stress statistics of the A1~A50 sample points are shown in Table 2. In order to quantitatively measure the variation of the resistance of the corroded component with the degree of corrosion, the ratio of the current stress value σ 1 to the design stress value σ 2 is used as the metric index of the resistance attenuation characteristics of the corroded component, which is recorded as $J=(\sigma 2/\sigma 1)\times 100\%$. The resistance attenuation J of A1~A₅₀ sample points is shown in Table 2.

2.2 Disease degree in the corroded area

For the corrosion morphology area of the main beam of the gate, the degree of corrosion disease at each sample point was clarified according to the comprehensive evaluation method. Taking the A_7 sample point as an example, its coordinates are (340,180), the radius of the affected neighborhood R=13.85mm is determined by the 1σ principle, the number of unit points is n=603, and a total of 15075 LBP₁₆² values identify the geometric morphology information of the corrosion area, and the relative morphology metrics of the corrosion area are mastered: corrosion rate u_1 =7.179%, corrosion rate u_2 =0.0323 mm/a, and corrosion distribution u_3 =81.1%. According to the half-trapezoidal function of Eq. 3, the evaluation factor z_{ij} is normalized to determine the

fuzzy evaluation matrix Z, as shown in Eq. 4.

$$Z = \begin{vmatrix} 0 & 0.876 & 1 & 0.124 & 0 \\ 0 & 0.882 & 1 & 0.118 & 0 \\ 0 & 0 & 0.556 & 1 & 0.444 \end{vmatrix}$$
 (4)

According to the importance of the corrosion morphology index, the weight vector $W=(0.4285,\,0.4285,\,0.143)$ was determined by expert voting, and the comprehensive evaluation of multi-factor index was calculated $Y=W\cdot Z$ (0,0.753,0.9636,0.246,0.063. According to the principle of maximum membership, the maximum membership degree of comprehensive multi-factor evaluation was 0.9636, and finally it was clear that the corrosion area was a tertiary corrosion disease. Other sample points are similar to this to identify the extent of disease in the corroded area, as shown in Table 2.

2.3 Test data analysis

In order to better grasp the intrinsic correlation characteristics of the $A_1 \sim A_{50}$ sample point data, according to the bearing test data shown in Table 2, the scatter plot of the resistance attenuation index J relative to the degree of corrosion disease of the corroded components was established, and the regression curve (fitting degree of 0.91) was fitted according to the least squares method, as shown in Fig. 6.

Table 2: Bearing test data of finite element components

Sample	(x,y)	R/mm	Disease grade	σ1/MPa	σ2/MPa	J/%
A1	380,230	15.76	IV	102.4	77.02	75.21
A2	380,180	16.24	V	118.74	76.9	64.76
A3	380,130	10.98	IV	100.03	76.98	76.96
A4	380,80	13.85	III	88.64	77.08	86.96
A5	380,30	16.72	V	138.13	76.78	55.59
A6	340,230	10.98	IV	104.88	76.92	73.34
A7	340,180	13.85	IV	94.84	77.0	81.19
A8	340,130	14.33	V	134.9	77.08	57.14
A9	340,80	15.29	IV	104.06	77.04	74.04
A10	340,30	14.8	III	88.3	76.94	87.14
A11	300,230	11.46	II	82.19	76.78	93.41
A12	300,180	10.89	I	78.31	76.96	98.28
A13	300,130	15.76	I	78.71	77.18	98.05
A14	300,80	13.86	I	78.09	76.96	98.55
A15	300,30	14.83	IV	92.47	76.56	82.8
A16	260,230	13.37	V	110.27	76.62	69.48
A17	260,180	12.91	II	80.37	76.94	95.73
A18	260,130	13.55	II	81.57	77.36	94.84
A19	260,80	13.76	II	79.82	77.1	96.59
A20	260,30	12.43	IV	97.15	76.72	78.97
A21	220,230	10.52	IV	97.14	76.18	78.43
A22	220,180	11.23	V	128.1	76.96	60.08
A23	220,130	12.63	IV	98.57	77.82	78.95
A24	220,80	10.36	V	132.06	77.32	58.55
A25	220,30	12.55	III	85.22	76.44	89.69
A26	180,230	13.37	IV	92.1	75.5	81.97
A27	180,180	14.11	I	79.22	77.32	97.6
A28	180,130	15.12	III	88.72	78.12	88.06
A29	180,80	13.68	IV	92.58	77.62	83.84
A30	180,30	14.12	III	85.3	76.04	89.15
A31	140,230	13.52	IV	89.27	75.0	84.02
A32	140,180	14.66	III	88.72	77.46	87.31
A33	140,130	13.28	III	87.69	78.06	89.02

A34	140,80	14.52	II	80.3	77.42	96.41
A35	140,30	14.87	III	82.88	75.3	90.86
A36	100,230	11.36	III	84.14	74.16	88.14
A37	100,180	13.65	III	86.71	76.92	88.71
A38	100,130	14.02	III	84.01	76.98	91.63
A39	100,80	14.36	IV	92.87	77.06	82.97
A40	100,30	13.69	III	82.29	75.28	91.48
A41	60,230	14.47	III	82.58	75.24	91.11
A42	60,180	13.98	V	113.49	75.5	66.52
A43	60,130	15.36	III	84.24	73.82	87.63
A44	60,80	14.56	II	78.58	74.86	95.26
A45	60,30	15.64	IV	96.96	76.7	79.11
A46	20,230	13.55	IV	107.72	81.34	75.51
A47	20,180	13.13	V	101.97	68.92	67.59
A48	20,130	14.01	V	101.74	67.16	66.01
A49	20,80	13.26	V	97.31	69.6	71.52
A50	20,30	13.42	IV	96.9	78.08	80.58

Note: (x,y) is the coordinate position of the sample point; R is the radius of the neighborhood affected by specimen pitting corrosion; $\sigma 1$ is the current stress value; $\sigma 2$ is the design stress value; $J=(\sigma 2/\sigma 1)\times 100\%$, which is the resistance attenuation index.

- (1) The resistance attenuation index of the corroded components is obvious with the degree of corrosion disease, and the maximum resistance attenuation index in the area with serious corrosion disease decreases by more than 44.41%, which should be reinforced or updated in time to ensure the safety of the structure.
- (2) The resistance attenuation index of the corroded

component shows significant discrete with the development of the degree of corrosion disease, and the more serious the corrosion disease, the greater the uncertainty of the resistance performance of the corroded component, with an uncertainty interval of more than 15.94%, which is manifested as a huge uncertainty of the in-service safety bearing of the project.

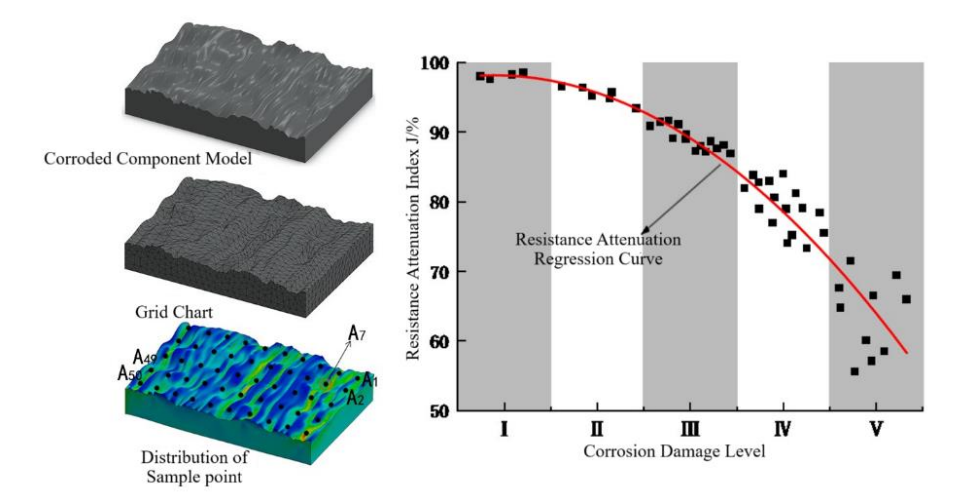


Fig 6: Distribution of component stress and fitting curve of resistance attenuation

3 Conclusion

- (1) Based on the image recognition technology of LBP algorithm, the image identification and optimization of corroded components were optimized, and the corrosion morphology information such as the identification unit points and LBP_{16}^2 values of the component images were successfully extracted, and the corrosion rate, corrosion rate and corrosion distribution factor indexes were established, so as to realize the quantitative identification and evaluation of the disease degree in the corrosion area.
- (2) Through the reconstruction of the model of the corroded component and the analysis of the finite element bearing test, the influence law of the corrosion disease of the corroded component on the attenuation of the resistance is clarified, and the resistance attenuation index of the corroded component is obvious with the degree of corrosion disease, and the maximum resistance attenuation index in the area

with serious corrosion disease decreases by more than 44.41%, and the resistance performance shows obvious discreteness, which is manifested in the sharp weakening of the bearing capacity of the component and the uncertainty of the safety of the in-service project. Therefore, it is necessary to pay close attention to the severely corroded components in the region to prevent the occurrence of engineering disasters.

References

- 1. Ang AH-S, Tang WH. Probability Concepts in Engineering: Emphasis on Applications to Civil and Environmental Engineering. Hoboken, New Jersey: John Willey & Sons Inc.; c2007.
- 2. Chen SS, Wang HX, Jiang H, Liu Y-N, Liu Y-X, Lv X-X. Risk assessment of corroded casing based on analytic hierarchy process and fuzzy comprehensive evaluation. Petroleum Science. 2021;18:591-602.

- 3. Dheepak G, Vaishali D. Brain tumor classification: a novel approach integrating GLCM, LBP and composite features. Frontiers in Oncology. 2024;13:1248452.
- 4. Granata RD, Wilson JC, Fisher JW. Assessing corrosion on steel structures using corrosion coulometer. Journal of Infrastructure Systems. 1996;2(3):139-144.
- Jarwar AR, Iqbal D, Mujahid M. The dynamics of Pakistan's renewable energy sector: tidal energy potential; a literature review. South Asian Research Journal of Engineering and Technology. 2023;5(6):94-101.
- 6. Li A, Ma H, Xu S. Three-dimensional morphology and watershed-algorithm-based method for pitting corrosion evaluation. Buildings. 2022;12(11):1908.
- 7. Li L, Gu J, Wu D. Mechanism analysis of rural residents' participation in green energy transition: A community-level case study in Nanjing, China. Heliyon. 2024;10(13).
- 8. Liu Y, Xu K, Xu J. An improved MB-LBP defect recognition approach for the surface of steel plates. Applied Sciences. 2019;9(20):4222.
- 9. Lu Y, Liu Y, Zhang D, Cao Z, Fu X. Chaotic characteristic analysis of spillway radial gate vibration under discharge excitation. Applied Sciences. 2023;14(1):99.
- 10. Mujahid M, Iqbal D, Rehman A, Abbas K. To secure your paper as per UGC guidelines we are providing an electronic bar code.
- 11. Patil PB, Shinde J. LBP based watermarking scheme for image tamper detection and recovery. International Journal of Computer Applications. 2015;975:8887.
- Saeedikhani M. Finite element method for modelling and mechanistic studies of corrosion under thin electrolytes. In: Advances in Corrosion Modelling. Springer; 2024. p. 189-215.
- 13. Song Y, Sa J, Luo Y, Zhang Z. A comprehensively improved local binary pattern framework for texture classification. Multimedia Tools and Applications. 2024:1-26.
- 14. Todd RV. Spillway tainter gate failure at Folsom Dam, California. In: Waterpower'99: Hydro's Future: Technology, Markets, and Policy; c1999. p. 1-10.
- 15. Wageh M, Amin KM, Zytoon A, Ibrahim M. Brain tumor detection based on a combination of GLCM and LBP features with PCA and IG. International Journal of Computers and Information. 2023;10(2):43-53.
- 16. Zeng S, Gu S, Ren S, Gu Y, Kong C, Yang L. A modeling method for finite element analysis of corroded steel structures with random pitting damage. Buildings. 2022;12(11):1793.
- 17. Liu GW, Jiang HR, Zhang YF, Wang W. 基于LBP特征 的人民币水印图像的识别与检测. 机电产品开发与创新. 2022;35(5):145-148.
- 18. **水工**钢闸门和启闭机安全检测技术规程. In: DL/T 835-2003; c2003.